2012 IEEE International Conference on Robotics and Automation
RiverCentre, Saint Paul, Minnesota, USA
May 14-18, 2012

# 3-D Mutual Localization with Anonymous Bearing Measurements

Marco Cognetti, Paolo Stegagno, Antonio Franchi, Giuseppe Oriolo, Heinrich H. Bülthoff

*Abstract*— **We present a decentralized algorithm for estimating mutual 3-D poses in a group of mobile robots, such as a team of UAVs. Our algorithm uses bearing measurements reconstructed, e.g., by a visual sensor, and inertial measurements coming from the robot IMU. Since identification of a specific robot in a group would require visual tagging and may be cumbersome in practice, we simply assume that the bearing measurements are anonymous. The proposed localization method is a non-trivial extension of our previous algorithm for the 2-D case [1], and exhibits similar performance and robustness. An experimental validation of the algorithm has been performed using quadrotor UAVs.**

## I. Introduction

In the last ten years, multi-agent systems have been widely studied in view of the potential increase in autonomy, versatility and robustness provided by decentralization. Mutual localization of the agents is one of the main capabilities needed to achieve those desirable features. In fact, tasks as cooperative exploration [2], formation control [3], connectivity maintenance [4], distributed estimation [5], cooperative transportation [6], coverage and sensing [7], [8], require each agent to possess some degree of knowledge about the poses of the others. If each agent is equipped with its own attached frame, one may define *Relative Mutual Localization* (RML) as the problem of estimating the change of coordinates among the agents' moving frames.

Many authors have dealt with the problem of estimating the poses of the agents in a *common* fixed frame [9], [10], [11], [12], [13], showing that the ability of sensing each other can be used to improve the localization accuracy of the entire system. In the literature, this kind of approach is called *Cooperative Localization*. Note that agreeing on a common fixed frame already implies a form of centralized consensus between the agents. Other works have studied observability in RML, showing the minimal sets of data needed to determine the robot-to-robot 3-D relative pose [14], and proposing suitable estimators [15], [16].

Most of the previous works assume that robot-to-robot measurements come with the identity of the measured robot, or equivalently that the estimation is performed *pairwise*. In [17], we have addressed the problem of 2-D RML with anonymous position measurements plus odometric data, the rationale being that the capability of achieving mutual localization with anonymous measurements actually increases the level of decentralization, widens the field of applicability and adds flexibility to the system. In that paper, we proposed a two-phase localization system composed by (1) a multiple registration algorithm that computes all the possible changes of coordinates among the agents' relative frames using geometrical arguments to invert the measurement map (2) a bank of particle filters to account for the uncertainty and ambiguity of the process (see also [18]). In [1], we have considered an extension to the case of bearing-only (rather than range-and-bearing) measurements, to allow the use of non-depth sensors such as simple cameras.

The objective of this paper is to extend our previous work to address the case of 3-D RML using anonymous bearing measurements. This would extend the benefits of our previous approach to a much wider class of systems, including aerial and submarine vehicles, as well as wheeled robots on 3-D surfaces. As we shall see, the extension to the 3-D case is however non-trivial, mainly due to the necessity of developing a completely new multiple registration algorithm to take into account (and to take advantage of) the increased dimension of the configuration space. Moreover, changing the vehicle model as well as the proprioceptive sensor equipments (from encoder-based odometry to inertial measurements) requires the redesign of the particle filters.

The paper is organized as follows. In Section II we formally introduce the considered mutual localization problem, while in Section III we describe our solution. Experimental results on a team of quadrotor UAVs are presented in Section IV, and some conclusions are given in Section V.

## II. Problem Formulation

Throughout this section, refer to Fig. 1 for illustration. Consider a system of $n$ robots $A_1, \ldots, A_n$, with $n$ unknown (hence, it may vary during the operation). Denote by $K = \{1, \ldots, n\}$ the set of robot indices, and let $K_i = K/\{i\}$. Each robot is a rigid body in $\mathbb{R}^3$. Denote by $\mathcal{W} : \{O_\mathcal{W}, X_\mathcal{W}, Y_\mathcal{W}, Z_\mathcal{W}\}$ and $\mathcal{B}_i : \{O_{\mathcal{B}_i}, X_{\mathcal{B}_i}, Y_{\mathcal{B}_i}, Z_{\mathcal{B}_i}\}$, respectively, the inertial (world) frame and the body frame attached to the center of mass of $A_i$. Body frames conform to the North-East-Down (NED) convention, as common in the aerospace field. The configuration of $A_i$ is represented by the position ${}^\mathcal{W}p_{\mathcal{B}_i} \in \mathbb{R}^3$ of the origin of $\mathcal{B}_i$ in $\mathcal{W}$ and the rotation matrix ${}^\mathcal{W}R_{\mathcal{B}_i} \in SO(3)$ between $\mathcal{W}$ and $\mathcal{B}_i$. Denote with $R_X(\cdot), R_Y(\cdot), R_Z(\cdot)$ the canonical rotation matrices about the axes $x, y, z$ respectively. Then ${}^\mathcal{W}R_{\mathcal{B}_i}$ can be written as ${}^\mathcal{W}R_{\mathcal{B}_i} = R_Z(\psi_{\mathcal{B}_i})R_Y(\theta_{\mathcal{B}_i})R_X(\phi_{\mathcal{B}_i})$, where

M. Cognetti, P. Stegagno and G. Oriolo are with the Dipartimento di Ingegneria Informatica, Automatica e Gestionale, Università di Roma La Sapienza, Roma, Italy. E-mail: marco.cognetti@gmail.com, stegagno@dis.uniroma1.it, oriolo@dis.uniroma1.it

A. Franchi is with the Max Plank Institute for Biological Cybernetics, Tübingen, Germany. E-mail: antonio.franchi@tuebingen.mpg.de

H. H. Bülthoff is with the Max Planck Institute for Biological Cybernetics, Tübingen, Germany, and with the Department of Brain and Cognitive Engineering, Korea University, Seoul, Korea. E-mail: hhb@tuebingen.mpg.de

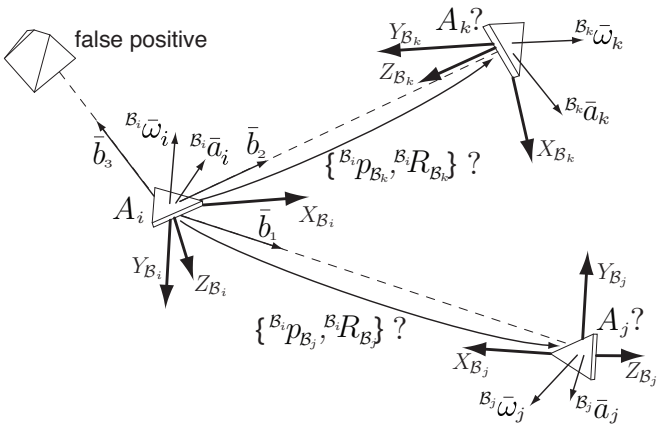


Fig. 1: 3-D mutual localization with anonymous bearing measurements. Robots (triangles) are shown with their attached frame and IMU measurements (angular velocity and acceleration). Robot $A_i$ detects two actual robots whose identities are unknown (hence the question marks) plus one false positive, and accordingly collects three anonymous bearing measurements.

$\psi_{\mathcal{B}_i}, \theta_{\mathcal{B}_i}, \phi_{\mathcal{B}_i} \in \mathbb{S}^1$ are the *yaw*, *pitch*, and *roll* angles of $A_i$, respectively, and $\mathbb{S}^1$ denotes the unit circle. The derivative of ${}^{\mathcal{W}}R_{\mathcal{B}_i}$ is ${}^{\mathcal{W}}\dot{R}_{\mathcal{B}_i} = [{}^{\mathcal{W}}\omega_{\mathcal{B}_i}]_\times {}^{\mathcal{W}}R_{\mathcal{B}_i}$, where

$$ {}^{\mathcal{W}}\omega_{\mathcal{B}_i} = \begin{pmatrix} {}^{\mathcal{W}}p_i \\ {}^{\mathcal{W}}q_i \\ {}^{\mathcal{W}}r_i \end{pmatrix}, \quad [{}^{\mathcal{W}}\omega_{\mathcal{B}_i}]_\times = \begin{pmatrix} 0 & -{}^{\mathcal{W}}r_i & {}^{\mathcal{W}}q_i \\ {}^{\mathcal{W}}r_i & 0 & {}^{\mathcal{W}}p_i \\ {}^{\mathcal{W}}q_i & -{}^{\mathcal{W}}p_i & 0 \end{pmatrix}, $$

and ${}^{\mathcal{W}}\omega_{\mathcal{B}_i}$ is the angular velocity in world frame.

Since we are interested in mutual localization among robots, define the following relative quantities

$$ {}^{\mathcal{B}_i}p_{\mathcal{B}_j} = {}^{\mathcal{W}}R_{\mathcal{B}_i}^T({}^{\mathcal{W}}p_{\mathcal{B}_j} - {}^{\mathcal{W}}p_{\mathcal{B}_i}) \tag{1} $$

$$ {}^{\mathcal{B}_i}R_{\mathcal{B}_j} = {}^{\mathcal{W}}R_{\mathcal{B}_i}^T {}^{\mathcal{W}}R_{\mathcal{B}_j} \tag{2} $$

and denote by ${}^{\mathcal{B}_i}x_{\mathcal{B}_j} = \{{}^{\mathcal{B}_i}p_{\mathcal{B}_j}, {}^{\mathcal{B}_i}R_{\mathcal{B}_j}\}$ the *full relative pose* between $A_i$ and $A_j$.

Each robot $A_i$ is equipped with a *motion detector*, such as an Inertial Measurement Unit (IMU), that provides measurements ${}^{\mathcal{B}_i}\bar{a}_i, {}^{\mathcal{B}_i}\bar{\omega}_i$ of its proper acceleration ${}^{\mathcal{B}_i}a_i$ and angular velocity ${}^{\mathcal{B}_i}\omega_i$ in body frame, given by

$$ {}^{\mathcal{B}_i}a_i = {}^{\mathcal{W}}R_{\mathcal{B}_i}^T({}^{\mathcal{W}}\ddot{p}_{\mathcal{B}_i} - g\, e_3) \tag{3} $$

$$ {}^{\mathcal{B}_i}\omega_i = {}^{\mathcal{W}}R_{\mathcal{B}_i}^T {}^{\mathcal{W}}\omega_{\mathcal{B}_i} \tag{4} $$

where $g$ is the gravity acceleration and $e_3 = (0\ 0\ 1)^T$.

In addition, $A_i$ comes with a *robot detector*, a sensor device which detects other robots and returns an anonymous measurement ${}^{\mathcal{B}_i}\bar{b}_{\mathcal{B}_j}$ of their *relative bearing*

$$ {}^{\mathcal{B}_i}b_{\mathcal{B}_j} = {}^{\mathcal{W}}R_{\mathcal{B}_i}^T \frac{{}^{\mathcal{W}}p_{\mathcal{B}_j} - {}^{\mathcal{W}}p_{\mathcal{B}_i}}{\|{}^{\mathcal{W}}p_{\mathcal{B}_j} - {}^{\mathcal{W}}p_{\mathcal{B}_i}\|} \in \mathbb{S}^2 \tag{5} $$

that is, the unit-norm vector in $\mathbb{R}^3$ pointing toward the center of mass[1] of $A_j$, expressed in $\mathcal{B}_i$. The measurement ${}^{\mathcal{B}_i}\bar{b}_{\mathcal{B}_j}$ is available whenever ${}^{\mathcal{B}_i}p_{\mathcal{B}_j} \in D_p$, the *perception set* attached to the robot.

In addition to being subject to false positives (due to objects that look like robots) and false negatives (due to occlusions), relative bearing measurements do not contain the identity of the measured robot (see Fig. 1). Therefore, the output of the robot detector is a set $B_{\mathcal{B}_i}$ of measurements whose ordering has no relation to the robot indexing; in addition, each measurement may or not refer to an actual robot. For this reason, in the following, relative bearing measurements will be generically referred to as *features*.

The equipment of each robot is completed by a *communication module* that can send/receive data to/from any other robot contained in a *communication set* $D_c$ around itself. We assume that $D_p \subset D_c$, so that if $A_i$ can detect $A_j$ it can also communicate with it. Each message by $A_i$ is composed by: (1) the robot signature (the index $i$), (2) the transformed acceleration measurement $\hat{a}_i$, (3) the transformed feature set $\hat{B}_i$, and (4) the partial estimates $\hat{\phi}_{\mathcal{B}_i}, \hat{\theta}_{\mathcal{B}_i}, \hat{\dot{\psi}}_i$. The definition of $\hat{a}_i, \hat{B}_i, \hat{\phi}_{\mathcal{B}_i}, \hat{\theta}_{\mathcal{B}_i}, \hat{\dot{\psi}}_i$ is given in Sect. III.

From now on, we consider the relative localization problem from the viewpoint of the generic robot $A_i$. Denote with $N_i$ the *neighbors* of $A_i$, i.e., the set of robots from which it is receiving communication. In a probabilistic framework, the RML problem with anonymous bearing measurements requires the generic robot $A_i$ to compute its belief about the relative poses of robots that are or have been its neighbors, using inertial and bearing measurements coming from its own sensory equipment or obtained via communication. In particular, using the superscripts $t$ and $1:t$ to denote the value of a variable at time $t$ and the history of its values at times $1, 2, \ldots, t$, we can formulate the following problem.

*Problem 1: (Probabilistic RML with anonymous bearing measurements)* For $t = 1, 2, \ldots$ and $j \in N_i^{1:t}$, compute the *belief* $\mathrm{bel}({}^{\mathcal{B}_i}x_{\mathcal{B}_j}) = P({}^{\mathcal{B}_i}x_{\mathcal{B}_j}^t \mid {}^{\mathcal{B}_i}\bar{a}_i^{1:t}, {}^{\mathcal{B}_i}\bar{\omega}_i^{1:t}, B_{\mathcal{B}_i}^{1:t}, \{{}^{\mathcal{B}_j}\bar{a}_j^\tau, {}^{\mathcal{B}_j}\bar{\omega}_j^\tau, B_{\mathcal{B}_j}^\tau\}_{j \in N_i^\tau, \tau=1,\ldots,t})$.

## III. 3-D Pose Estimation

For $k \in K$, denote with $\mathcal{C}_k = \{O_{\mathcal{C}_k}, X_{\mathcal{C}_k}, Y_{\mathcal{C}_k}, Z_{\mathcal{C}_k}\}$ the frame having the same origin as $\mathcal{B}_k$ and such that ${}^{\mathcal{W}}R_{\mathcal{C}_k} = R_Z(\psi_{\mathcal{B}_k})$. Being ${}^{\mathcal{C}_k}R_{\mathcal{B}_k} = R_Y(\theta_{\mathcal{B}_k})R_X(\phi_{\mathcal{B}_k})$, we have

$$ {}^{\mathcal{C}_k}R_{\mathcal{B}_k} = \begin{pmatrix} c\theta_{\mathcal{B}_k} & s\phi_{\mathcal{B}_k}s\theta_{\mathcal{B}_k} & c\phi_{\mathcal{B}_k}s\theta_{\mathcal{B}_k} \\ 0 & c\phi_{\mathcal{B}_k} & -s\phi_{\mathcal{B}_k} \\ -s\theta_{\mathcal{B}_k} & s\phi_{\mathcal{B}_k}c\theta_{\mathcal{B}_k} & c\phi_{\mathcal{B}_k}c\theta_{\mathcal{B}_k} \end{pmatrix}. \tag{6} $$

The scheme of our estimation algorithm is shown in Fig. 2. We split Problem 1, i.e., the problem of estimating ${}^{\mathcal{B}_i}x_{\mathcal{B}_j}$, $j \in N_i^{1:t}$, in two subproblems.

*Estimation of pitch and roll:* Each $A_k$ independently obtains estimates $\hat{\phi}_{\mathcal{B}_k}$ and $\hat{\theta}_{\mathcal{B}_k}$ of its roll and pitch angles using the motion detector measurements ${}^{\mathcal{B}_k}\bar{a}_k, {}^{\mathcal{B}_k}\bar{\omega}_k$. This is achieved using a complementary filter (see [19], [20]). $A_k$ can then compute an estimate ${}^{\mathcal{C}_k}\hat{R}_{\mathcal{B}_k}$ of ${}^{\mathcal{C}_k}R_{\mathcal{B}_k}$ using (6).

*Estimation of the reduced relative pose:* We solve a problem which is simpler than Problem 1, and consists in retrieving the identities of the relative bearing measurements

[1] A measurement of (5) can be obtained, for example, by using a feature tracking algorithm on the images provided by a calibrated camera mounted on the robot. The choice and description of the tracking algorithm belongs to the computer vision field and is outside the scope of this paper.

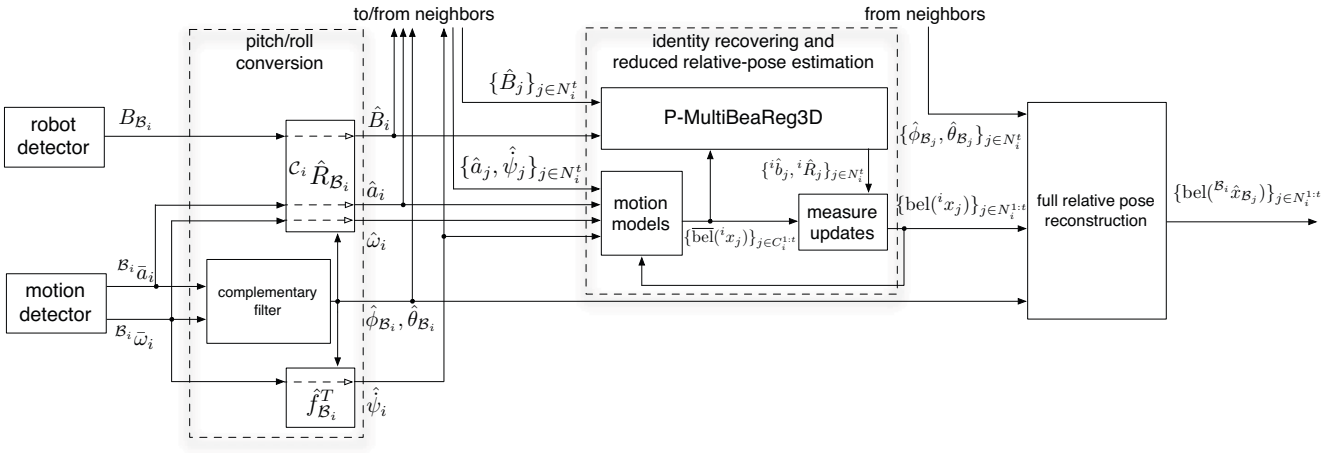


Fig. 2: Scheme of the mutual localization system that runs on the generic robot $A_i$.

and estimating a *reduced relative pose* ${}^i x_j = \{{}^i p_j, {}^i R_j\}$, $j \in N_i^{1:t}$, where

$$ {}^i p_j = {}^{\mathcal{W}} R_{\mathcal{C}_i}^T ({}^{\mathcal{W}} p_{\mathcal{C}_j} - {}^{\mathcal{W}} p_{\mathcal{C}_i}) \tag{7} $$

$$ {}^i R_j = R_Z(\psi_{\mathcal{B}_i})^T R_Z(\psi_{\mathcal{B}_j}). \tag{8} $$

Denote by ${}^i \hat{x}_j = \{{}^i \hat{p}_j, {}^i \hat{R}_j\}$ the corresponding estimates.

Once both subproblems are solved, it is immediate to compute an estimate ${}^{\mathcal{B}_i} \hat{x}_{\mathcal{B}_j} = \{{}^{\mathcal{B}_i} \hat{p}_{\mathcal{B}_j}, {}^{\mathcal{B}_i} \hat{R}_{\mathcal{B}_j}\}$ of the relative pose required by Problem 1 by setting ${}^{\mathcal{B}_i} \hat{p}_{\mathcal{B}_j} = {}^{\mathcal{C}_i} \hat{R}_{\mathcal{B}_i}{}^T \, {}^i \hat{p}_j$ and ${}^{\mathcal{B}_i} \hat{R}_{\mathcal{B}_j} = {}^{\mathcal{C}_i} \hat{R}_{\mathcal{B}_i}{}^T \, {}^i \hat{R}_j$.

For the estimation of the reduced relative pose ${}^i x_j$, rather than the motion and robot detector measurements (3–5) we use the corresponding quantities in the $\mathcal{C}_i$ frame

$$ a_i = {}^{\mathcal{W}} R_{\mathcal{C}_i}^T ({}^{\mathcal{W}} \ddot{p}_{\mathcal{C}_i} - g e_3) \tag{9} $$

$$ \omega_i = {}^{\mathcal{W}} R_{\mathcal{C}_i}^T \, {}^{\mathcal{W}} \omega_{\mathcal{C}_i} \tag{10} $$

$$ {}^i b_j = \frac{{}^i p_j}{\|{}^i p_j\|} = {}^{\mathcal{W}} R_{\mathcal{C}}^T \frac{{}^{\mathcal{W}} p_{\mathcal{C}_j} - {}^{\mathcal{W}} p_{\mathcal{C}_i}}{\|{}^{\mathcal{W}} p_{\mathcal{C}_j} - {}^{\mathcal{W}} p_{\mathcal{C}_i}\|}. \tag{11} $$

Using the roll and pitch estimates from the complementary filter we have

$$ \hat{a}_i = {}^{\mathcal{C}_i} \hat{R}_{\mathcal{B}_i} \, {}^{\mathcal{B}_i} \bar{a}_i \tag{12} $$

$$ \hat{\omega}_i = {}^{\mathcal{C}_i} \hat{R}_{\mathcal{B}_i} \, {}^{\mathcal{B}_i} \bar{\omega}_i \tag{13} $$

$$ {}^i \hat{b}_j = {}^{\mathcal{C}_i} \hat{R}_{\mathcal{B}_i} \, {}^{\mathcal{B}_i} \bar{b}_j. \tag{14} $$

We emphasize that the estimates of the transformed relative bearings ${}^i \hat{b}_j$ are still anonymous. In fact only the set

$$ \hat{B}_i = \{{}^{\mathcal{C}_i} \hat{R}_{\mathcal{B}_i} b \,|\, b \in B_{\mathcal{B}_i}\} $$

is actually available at every time $t$. In addition, the system uses an estimate estimate $\hat{\dot{\psi}}_{\mathcal{B}_k}$ of the yaw rate, which is computed plugging the roll and pitch estimates into the formula

$$ \dot{\psi}_{\mathcal{B}_k} = \begin{pmatrix} 0 & \dfrac{\sin \phi_{\mathcal{B}_k}}{\cos \theta_{\mathcal{B}_k}} & \dfrac{\cos \phi_{\mathcal{B}_k}}{\cos \theta_{\mathcal{B}_k}} \end{pmatrix} {}^{\mathcal{B}_k} \bar{\omega}_k = f_{\mathcal{B}_k}^T \, {}^{\mathcal{B}_k} \bar{\omega}_k, \tag{15} $$

where $f_{\mathcal{B}_k}^T =$ is the co-vector which transforms the angular velocity in body frame into the yaw rate.

This leads to the following reformulation of Problem 1.

*Problem 2:* For $t = 1, 2, \ldots$ and $j \in N_i^{1:t}$, compute the *belief* $\mathrm{bel}({}^i x_j) = P({}^i x_j^t |\, \hat{a}_i^{1:t}, \hat{\omega}_i^{1:t}, \hat{B}_i^{1:t}, \hat{\dot{\psi}}_i^{1:t}, \hat{\phi}_{\mathcal{B}_i}^{1:t}, \hat{\theta}_{\mathcal{B}_i}^{1:t}, \{\hat{a}_j^\tau, \hat{\dot{\psi}}_j^\tau, \hat{B}_j^\tau, \hat{\phi}_{\mathcal{B}_j}^\tau, \hat{\theta}_{\mathcal{B}_j}^\tau\}_{j \in N_i^\tau, \tau = 1, \ldots, t})$.

In order to solve Problem 2 we need to recover: (1) the identities of the measurements in $\hat{B}_i$, (2) the relative orientations ${}^i R_j$, and (3) the relative distances $\|{}^i p_j\|$. In analogy with [1], where the 2-D case has been addressed, we adopt a two-step approach.

First, a multiple registration algorithm (P-MultiBeaReg3D, described in Sect. III-A) is used to retrieve the identities in $\hat{B}_i$ and the ${}^i \hat{R}_j$ matrices. For every $j \in N_i$, the output of P-MultiBeaReg3D is a set of elements of $\mathbb{S}^2 \times SO(3)$ that represent our best guesses for ${}^i b_j$ and ${}^i R_j$, given the anonymous measurements $\hat{B}_i$, $\{\hat{B}_j\}_{j \in N_i}$, and the current belief about ${}^i x_j$. In parallel, for each $j \in N_i^{1:t}$, a Particle Filter (PF) is used to retrieve the distance $\|{}^i \hat{p}_j\|$, based on the output of P-MultiBeaReg3D and the inertial measurements in (12–13). The PFs are described in Sect. III-B.

### A. Identity and Mutual Orientation Recovering

P-MultiBeaReg3D is the probabilistic multiple registration algorithm run by $A_i$ at each time instant $t$ to feed the measurement update of the particle filters (see Fig. 2). In general, *registration* is the process of computing the relative pose between two or more different viewpoints of the same scene. In our case, since the 'scene' consists only of sets of bearing measurements, the scale of the relative poses cannot be recovered. In particular, given the sets of features $\hat{B}_i$, $\{\hat{B}_j\}_{j \in N_i}$ and the current beliefs $\{\overline{\mathrm{bel}}({}^i x_j)\}_{j \in N_i}$ computed by the particle filters through the motion model of the robots (see Fig. 2), P-MultiBeaReg3D derives an estimate of the relative bearing-orientation of $A_j$, $j \in N_i$, w.r.t. $A_i$.

A pseudo-code description of P-MultiBeaReg3D is given in Algorithm 1 and its basic steps are illustrated in Fig. 3. The underlying idea of this algorithm is to search first for all triangles in the scene and then to reconstruct the formation, joining the triangles found, up to a scaling factor.

**Algorithm 1**: P-MultiBeaReg3D

**input** : feature sets $\hat{B}_i$, $\{\hat{B}_j\}_{j\in N_i}$, beliefs $\overline{\text{bel}}\{{}^i x_j\}_{j\in N_i}$
**output**: relative bearing-orientation estimates

1 Identify triangles from the feature sets;
2 Rate triangles according to their 2- and 3-intersections and collect those above a certain threshold in a set $\mathcal{T}$;
3 Extract from $\mathcal{T}$ a maximal subset $\mathcal{T}_{\text{irr}}$ of irreconcilable triangles containing $A_i$;
4 Define *partial solution* each triangle in $\mathcal{T}_{\text{irr}}$ whose metric (17) is above a certain threshold;
5 **foreach** *partial solution* $S$ **do**
6 Expand $S$ with each triangle $T_m \in \mathcal{T}$ such that $S$ and $T_m$ have a common side, and $T_m \notin S$;
7 For each new partial solution, compute its 2- and 3-intersections and select solutions with rating above a threshold;
8 Select a maximal subset of irreconcilable solutions and set them as partial solutions for the next step;
9 Prune solutions whose metric (17) is under an adaptive threshold;
10 **if** *no new partial solution* **then** end branch;
11 **else goto** 5

Consider the situation in Fig. 3a, where four robots are arranges in a 'square' formation with the opposite vertices at the same height; the corresponding feature sets are shown in Fig. 3b. In this situation there is no vertical alignment among robots, i.e., no measurement in $\hat{B}_i \cup \{\hat{B}_j\}_{j\in N_i}$ is equal to $(0\,0\,\pm 1)^T$.

Note that each bearing measurement can be equivalently represented by an azimuth and zenith-distance pair. For example, a given bearing ${}^i\hat{b}_j$ can be represented by $({}^i\alpha_j, {}^i\zeta_j) \in [0, 2\pi) \times [0, \pi)$, since they are related by

$$ {}^i\hat{b}_j = (\sin{}^i\zeta_j \cos{}^i\alpha_j \;\; \sin{}^i\zeta_j \sin{}^i\alpha_j \;\; \cos{}^i\zeta_j)^T, \qquad (16)$$

where ${}^i\alpha_j$ and ${}^i\zeta_j$ are azimuth and zenith-distance angles, respectively. The projection of $\hat{B}_i$ on the $XY$ plane of $\mathcal{C}_i$ preserves only the azimuth information. Furthermore, each pair of azimuth angles in the same feature set (i.e., belonging to the same robot) can be equivalently represented by their difference. Note that the $XY$ planes (as well as the $Z$ axes) of the reference frames $\mathcal{C}_k, k = 1, 2, \ldots n$ are parallel to each other. Then, an azimuth angle difference represents a feasible internal angle of a planar triangle.

Consider now a triplet of robots that 'see' each other, e.g., $A_i$, $A_j$, $A_k$, and make $A_h$ 'disappear' for a moment, so that each robot in the triplet sees only two features, or equivalently one difference angle. Since the projection of a 3-D triangle on $\mathcal{C}_i$'s $XY$ plane[2] defines a planar triangle, the sum of the three difference angles must be $\pi$. The algorithm then scans all the possible triplets coming from different fature sets and looks for triplets of difference angles (one from each feature set) whose sum is $\pi$, with a certain tolerance. Each of these triplets defines a planar triangle; more precisely, it defines a class of equivalence, because the triangle is defined only up to a scaling factor. Note

[2]The same holds for every $\mathcal{C}_k$, since all $XY$ planes are parallel.

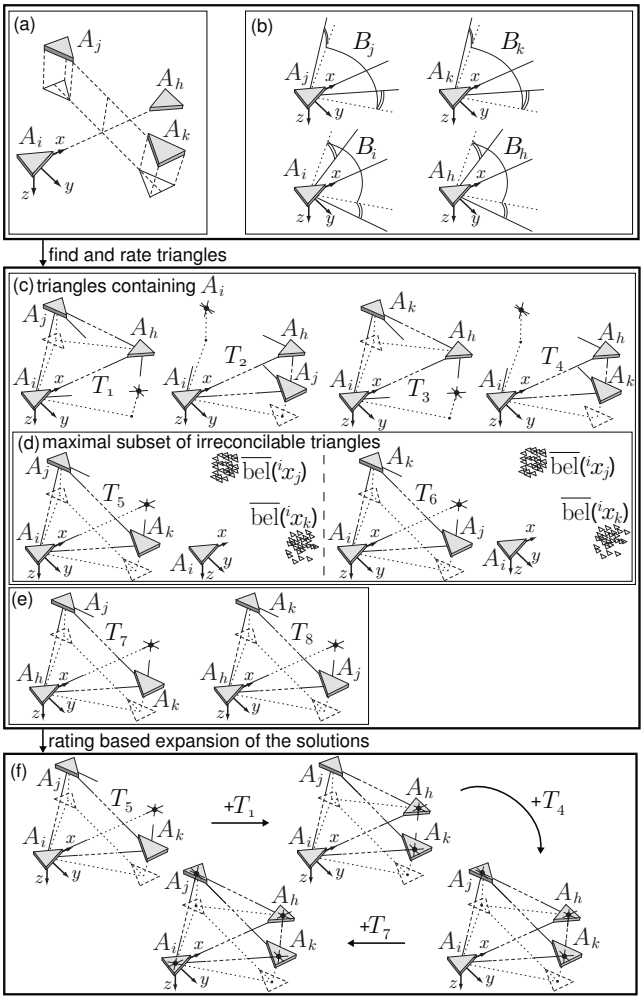


Fig. 3: Execution of P-MultiBeaReg3D in an ambiguous situation: (a) actual configuration (b) initial feature sets (c) triangle found in the first step containing the owner of the algorithm and their triple intersections (d) maximal subset of irreconcilable triangles and their comparison with the current belief (e) other triangles found in the first step of the algorithm and their triple intersections (f) expansion of the solution using the remaining triangles.

that a triangle encodes also the identity of the robots at its vertices. With respect to the 2-D case considered in [1], such triangles must satisfy also an additional condition. In fact, each azimuth angle comes with a zenith-distance angle associated. By building the triangle as explained, we are implying that a certain feature of a set is the equivalent of another feature of another set. Then, the sum of the zenith-distances of two associated bearings must be equal to $\pi$, with a certain tolerance.

When two robots in a triangle see another robot that is not the third vertex of the triangle, their feature sets will contain two intersecting rays, one for each set. We will call this a *2-intersection*. A triangle can also have *3-intersections*, when all three robots forming it see a fourth robot (e.g., $A_h$ in Fig. 3a). In particular a 3-intersection is equivalent to three 2-intersections. Based on this idea, the algorithm rates all the triangles by counting their 2-intersections and discards

those below a certain threshold. From the remaining set $\mathcal{T}$, a maximal subset $\mathcal{T}_{\text{irr}}$ is extracted of irreconcilable triangles containing $A_i$; two triangles are said to be *irreconcilable* if they associate the same robot to different features of the same set (e.g., $A_j$ in $T_1$ and $T_2$, Fig. 3c), or two different robots to the same feature (e.g., $A_j$ and $A_k$ in $T_1$ and $T_3$, Fig. 3c). The results of this process of triangle finding and rating are illustrated in Fig. 3c–e. In particular, Fig. 3c shows all the triangles having one 3-intersection and containing $A_i$; Fig. 3e shows all the triangles having one 3-intersection but not containing $A_i$. One choice for the maximal subset $\mathcal{T}_{\text{irr}}$ is shown in Fig. 3d.

The next step is aimed at validating the triangles in $\mathcal{T}_{\text{irr}}$ on the basis of the current belief about the pose of the robots. To this end, we use the metric function

$$P(\{{}^i\hat{b}_j, {}^i\hat{R}_j\}) = \int p(\{{}^i\hat{b}_j, {}^i\hat{R}_j\}|{}^ix_j)\overline{\text{bel}}({}^ix_j)d^ix_j \qquad (17)$$

where $\overline{\text{bel}}({}^ix_j)$ comes from the motion block of the particle filters. First, the scale of each triangle is computed so as to maximize this function; then, an adaptive thresholding of these maximum values is used to select the triangles that better fit the belief.

Each triangle of the $\mathcal{T}_{irr}$ set is the base of a branch of the algorithm and constitutes the partial solution at the first step of its branch. The partial solution of each branch is then iteratively expanded looking for triangles that have common edges with it (see Fig. 3f). Let $S$ be the partial solution (given as a collection of triangles, the change of coordinates between them and the total number of 2- and 3- intersections as rating) of a branch at a given step. Let $\mathcal{T}_{\mathcal{S}} = \{T_m, m = 1, \ldots, M\}$ be the set of the feasible triangles $T_m \in \mathcal{T}$ not yet in $S$ that have a common edge with one triangle in $S$. Then the algorithm builds a set of $M$ possible partial solutions for the next step expanding $S$ with $T_m, m = 1, \ldots, M$. Each solution is then rated by counting its total number of 2 and 3-intersections. Note that each matching of two 3-intersections generates a 4-intersection, that accounts for four 3-intersections as well as two matching 2-intersections generates a triple intersection. An $n$-intersection in general accounts for $n!/[(n-3)!3!]$ 3-intersections. A vertex of a triangle matching with a 3-intersection accounts for an additional 4-intersection, while adding a triangle that has all three vertexes already in the solution (but the triangle itself is not yet in the solution) accounts for an additional 4-intersection. Finally, the algorithm searches for triangles in $\mathcal{T}_S$ that are reconcilable with $S$. If a triangle in $\mathcal{T}_S$ is reconcilable with $S$, an additional 4-intersection is added, increasing the weight of the actual solution. In fact, the more triangles fit with the solution, the higher is the probability that it is correct. In the case of Fig. 3f, one obtains a partial solution joining triangle $T_5$ and $T_1$ whose weight account for two 4-intersections because of the triple intersection of each triangle will overlap on a vertex of the other triangle during the triangle fusion phase. The iterative addition of $T_4$ and $T_7$ results in the increase of the weight of the solution of this branch by other two four-intersections.

Then, as in the case of the triangle, the algorithm selects a subset of partial solution whose rating is above an adaptive threshold. Again, a maximal subset of irreconcilable partial solutions is selected and, among them, only the solutions that fit with the current belief according to equation (17) are used as partial solutions at following step, expanding a branch for each of them. The iterative process continues in each branch until $\mathcal{T}_{\mathcal{S}}$ becomes empty in that branch. The algorithm generates a new branch whenever an irreconcilable triangle is inserted in the solution, substituting the conflicting vertexes and expanding both solutions. In the end, each branch finds a solution, and the best of them are selected, once again with the intersection and likelihood criteria. Since each branch of the algorithm may in principle produce a different pair ${}^i\hat{b}_k, {}^i\hat{R}_k$ for each $A_k$, each with its own weight, the result is a list of such pairs for the generic robot $A_k$.

If two robots are vertically aligned (a zero-measure case) the algorithm is the same but looks for triangles considering the difference angles in the other bearing dimension, i.e., zenith-distance.

### *B. Relative Distance Estimation*

The generic robot $A_i$ runs one particle filter (PF$_j$) for each $A_j$ to retrieve the missing relative distance $\|{}^ip_j\|$. This is obtained by fusing the depthless quantities ${}^i\hat{b}_j, {}^i\hat{R}_j$ coming from P-MultiBeaReg3D with the metric informations provided by the IMUs of $A_i$ and $A_j$.

The equations of motion are

$$ {}^i\dot{p}_j = {}^iv_j \qquad (18)$$

$$ {}^i\dot{v}_j = {}^iR_j a_j - a_i + [\omega_i]_\times {}^iv_j \qquad (19)$$

$$ {}^i\dot{R}_j = ({}^iR_j[\omega_j]_\times - [\omega_i]_\times){}^iR_j \qquad (20)$$

where we denoted with ${}^iv_j$ the velocity of $O_{\mathcal{C}_j}$ in $\mathcal{C}_i$. Since

$${}^iR_j = R_Z(-\psi_{\mathcal{B}_i})R_Z(\psi_{\mathcal{B}_j}) = R_Z(\psi_{\mathcal{B}_j} - \psi_{\mathcal{B}_i}), \qquad (21)$$

we can replace (20) with

$${}^i\dot{\psi}_j = \dot{\psi}_{\mathcal{B}_j} - \dot{\psi}_{\mathcal{B}_i} = f_{\mathcal{B}_j}^{T\,\mathcal{B}_j}\omega_j - f_{\mathcal{B}_i}^{T\,\mathcal{B}_i}\omega_i, \qquad (22)$$

being ${}^i\psi_j = \psi_{\mathcal{B}_j} - \psi_{\mathcal{B}_i}$ and $f_{\mathcal{B}_i}^T, f_{\mathcal{B}_j}^T$ defined by (15), and compute ${}^iR_j$ in (19) from (21). Therefore the state of each particle in PF$_j$ is the 7-dimensional tuple ${}^i\chi_j = ({}^ip_j, {}^iv_j, {}^i\psi_j) \in \mathbb{R}^3 \times \mathbb{R}^3 \times \mathbb{S}^1$. The observability of the system is guaranteed by [16]. In particular, one can use the analysis in that paper to generate exciting trajectories.

The motion update step of PF$_j$ is obtained by plugging $\hat{a}_i, \hat{a}_j, \hat{\omega}_i, \hat{\dot{\psi}}_{\mathcal{B}_i}, \hat{\dot{\psi}}_{\mathcal{B}_j}$ in (18–22). The new state probability is predicted by means of the integration of the motion measurements with the knowledge of the measurement noise.

Coming to the measurement update step, note first that, at each $t$, the algorithm P-MultiBeaReg3D may return more than one solution per robot, i.e., more than one pair ${}^i\hat{b}_j, {}^i\hat{R}_j$, each solution rated on the basis of its uncertainty during the registration steps of the algorithm. For this reason, each solutions is approximated in PF$_j$ as a gaussian measurement with a covariance proportional to its uncertainty. Therefore,

Fig. 4: The quadrotor model used in our experiments.

the measurement model is given by the normalized sum of gaussians centered at the solutions of P-MultiBeaReg3D.

Denote with ${}^i\hat{\psi}_j$ the estimate of ${}^i\psi_j$ obtained from ${}^i\hat{R}_j$. The measurement update produces a rating of the predicted particles by using Bayes' law

$$P({}^i\chi_j|{}^i\hat{b}_j, {}^i\hat{\psi}_j) = NP({}^i\hat{b}_j, {}^i\hat{\psi}_j|{}^i\chi_j)P({}^i\chi_j), \tag{23}$$

where $N$ is a normalization factor.

We used separate beliefs $P({}^i\chi_j)$, with $j \in N_i^{1:t}$, instead of a single joint belief $P(\{{}^i\chi_j\}_{j\in N_i^{1:t}})$, based on the independence assumption, i.e., $P(\{{}^i\chi_j\}_{j\in N_i^{1:t}}) = \prod_{j\in N_i^{1:t}} P({}^i\chi_j)$. This assumption is true in a pure localization scenario, while in in certain situations it is only an acceptable approximation. In any case, $P(\{{}^i\chi_j\}_{j\in N_i^{1:t}})$ cannot be maintained due to its computational cost, as the dimension of its distribution grows exponentially with the number of robots.

A number of standard practical techniques have been used to improve the performance of the filter. For example, the initial prior distribution is generated using the first measurements. Moreover, we have reduced the frequency of the measurement update with respect to the motion update to guarantee the independence of subsequent measurements. Finally, we have used a Tustin integration to smooth the acceleration data coming from the motion detector.

## IV. Experimental Results

The proposed mutual localization system has been experimentally tested on a group of Mikrokopter quadrotors (http://www.mikrokopter.com, see Fig. 4) flying in an arena of $10 \times 12 \times 6$ m. We used an external motion capture system (http://www.vicon.com), whose precision is about 1 mm for translations and 1° for rotations, to obtain a ground truth.

As a motion detector, we used the IMU available on the microcontroller board, composed by one three-axis linear MEMS accelerometer plus three orthogonally mounted angular rate sensors. The microcontroller acquires these measurements at 400 Hz, and runs at the same frequency the complementary filter to recover the current roll and pitch. In particular, the estimate $\hat{\phi}_{\mathcal{B}_i}$ ($\hat{\theta}_{\mathcal{B}_i}$) of the roll (pitch) is computed by fusing the accelerometer measurement ${}^{\mathcal{B}_i}\bar{a}_{i_Y}$ (${}^{\mathcal{B}_i}\bar{a}_{i_X}$) with the gyroscope measurement ${}^{\mathcal{B}_i}\bar{\omega}_{i_X}$ (${}^{\mathcal{B}_i}\bar{\omega}_{i_Y}$). For

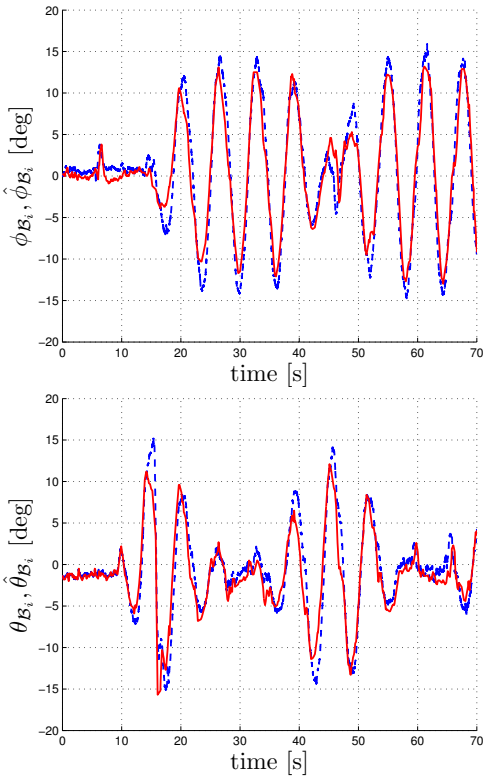


Fig. 5: Estimates (red) of the roll and pitch angles computed by the complementary filter w.r.t. ground truth values (blue) in a typical experiment.

our quadrotor, the dynamics of the filter is

$$\dot{\hat{\phi}}_{\mathcal{B}_i} = {}^{\mathcal{B}_i}\bar{\omega}_{i_Y} + k_{\phi_i}({}^{\mathcal{B}_i}\bar{a}_{i_Y} - \hat{\phi}_{\mathcal{B}_i})$$
$$\dot{\hat{\theta}}_{\mathcal{B}_i} = {}^{\mathcal{B}_i}\bar{\omega}_{i_X} + k_{\theta_i}({}^{\mathcal{B}_i}\bar{a}_{i_X} - \hat{\theta}_{\mathcal{B}_i}).$$

The typical performance of the filter is shown in Fig. 5; here, the mean error is 1.92° for roll and 2.67° for pitch.

Due to the limited memory and processing power of the microcontroller, the localization algorithm runs on a GNU-Linux machine to which $({}^{\mathcal{B}_i}\bar{a}_i, {}^{\mathcal{B}_i}\bar{\omega}_i, \hat{\phi}_{\mathcal{B}_i}, \hat{\theta}_{\mathcal{B}_i})$ are transmitted through a serial connection. This connection is slow (average rate 20 Hz with standard deviation 4 ms) and represents a bottleneck in our testbed but also a challenge for the localization algorithm.

The scaling factors for the IMU readings and the noise characteristics of ${}^{\mathcal{B}_i}\bar{a}_i, {}^{\mathcal{B}_i}\bar{\omega}_i$ have been identified via a preliminary statistical analysis conducted over a set of data collected with the quadrotor in simple hovering. In particular, the resolutions of the accelerometer and of the gyroscope are respectively $(0.019, 0.019, 0.019)$ m/s$^2$ and $(0.29, 0.29, 0.29)$ deg/s, while their variances are $(0.1, 0.1, 0.6)$ m/s$^2$ and $(0.64, 0.64, 1.12)$ deg/s. The large variance for the accelerometer is also due to the vibrations induced by the motors/propellers.

We simulated the behavior of an on-board robot detector by analytically computing the relative bearing from the ground truth via (5), adding to the azimuth and zenith-distance angles a zero-mean gaussian noise with standard

deviation of 5 deg (the noise typically observed in visual tracking experiments with the same system), and randomly introducing false positives and negatives.

The results of an experiment with 4 quadrotors starting in a square ambiguous configuration are shown in Fig. 6–7. In particular, the results refer to the mutual localization algorithm running on $A_1$. The 'best' particle has been used as estimate, because it shows a better behavior with respect to the average of the particles. This is due to the multiple registration algorithm that can return more than one solution for each robot. Another possible solution would be to make a clustering analysis on the particles. The plots in Fig. 6 show the errors on roll and pitch estimates computed by the complementary filters of all robots, plus the errors on azimuth, zenith-distance, distance and yaw estimates computed by the particle filters for $A_2$, $A_3$ and $A_4$ that run on $A_1$. Since the initial configuration is ambiguous, the initial errors are large. Moreover, the relative distances being initially unknown, the particles were purposely initialized at random relative distances with substantial mean error to test the ability of the algorithm to recover from such situation. As soon as the symmetry of the formation is broken and the robots have traveled enough, the localization algorithm is able to retrieve the correct relative distances. It should be noted that the convergence of the estimates is faster than in the 2-D case [1], thanks to the fact that the multiple registration algorithm more often returns a single solution.

The second experiment involves eight quadrotors and is aimed at testing the localization algorithm in the presence of false positives and false negatives. False negatives are simulated by randomly deleting a feature from the generic feature set $\hat{B}_k$ for up to 3 seconds; false positives are generated by quadrotors $A_7$ and $A_8$ that are detected by the others but do not communicate any information. The results of the mutual localization algorithm running on $A_1$, shown in Fig. 8–Fig. 9, confirm the robustness of the proposed method.

See the accompanying video for more illustrative clips of the experiments.

## V. Conclusions

We have presented a decentralized method for mutual localization in multi-agent systems using anonymous bearing measurements in a 3-D environment. This is a non trivial extension of our previous work [1] which assumes bearing measurements but in a planar setting. Here, the challenge was to extend our framework to $SE(3)$, using in addition a IMU (more noisy and less informative than wheel encoders) to estimate robot displacements. This led us to design an architecture that estimates relative poses as well as velocities among the robots. In comparison with [1], we also reduced the time needed to retrieve the missing distance information, thanks to an improved multiple registration algorithm and to the increased dimension of the environment. Experimental results on a team of quadrotor UAV confirm that the localization method is effective. In the future, we plan to apply the proposed approach to an heterogeneous multi-robot system.

## References


[1] P. Stegagno, M. Cognetti, A. Franchi, and G. Oriolo, "Mutual localization using anonymous bearing-only measures," in *2011 IEEE/RSJ Int. Conf. on Intelligent Robots and Systems*, San Francisco, CA, Sep. 2011, pp. 469–474.

[2] A. Howard, L. E. Parker, and G. S. Sukhatme, "Experiments with a large heterogeneous mobile robot team: Exploration, mapping, deployment and detection," *International Journal of Robotics Research*, vol. 25, no. 5-6, pp. 431–447, 2006.

[3] N. Michael and V. Kumar, "Planning and control of ensembles of robots with non-holonomic constraints," *International Journal of Robotics Research*, vol. 28, no. 8, pp. 962–975, 2009.

[4] P. Yang, R. A. Freeman, G. J. Gordon, K. M. Lynch, S. S. Srinivasa, and R. Sukthankar, "Decentralized estimation and control of graph connectivity for mobile sensor networks," *Automatica*, vol. 46, no. 2, pp. 390–396, 2010.

[5] P. Yang, R. A. Freeman, and K. M. Lynch, "Multi-agent coordination by decentralized estimation and control," *IEEE Trans. on Automatic Control*, vol. 53, no. 11, pp. 2480–2496, 2008.

[6] J. Fink, N. Michael, S. Kim, and V. Kumar, "Planning and control for cooperative manipulation and transportation with aerial robots," *International Journal of Robotics Research*, vol. 30, no. 3, 2010.

[7] M. Schwager, B. J. Julian, and D. Rus, "Optimal coverage for multiple hovering robots with downward facing cameras," in *2009 IEEE Int. Conf. on Robotics and Automation*, Kobe, Japan, May 2009, pp. 3515–3522.

[8] L. C. A. Pimenta, V. Kumar, R. C. Mesquita, and G. A. S. Pereira, "Sensing and coverage for a network of heterogeneous robots," in *47th IEEE Conf. on Decision and Control*, Cancun, Mexico, Dec. 2008, pp. 3947–3952.

[9] D. Fox, W. Burgard, H. Kruppa, and S. Thrun, "A probabilistic approach to collaborative multi-robot localization," *Autonomous Robots*, vol. 8, no. 3, pp. 325–344, 2000.

[10] S. I. Roumeliotis and G. A. Bekey, "Distributed multirobot localization," *IEEE Trans. on Robotics*, vol. 18, no. 5, pp. 781–795, 2002.

[11] A. Howard, M. J. Matarić, and G. S. Sukhatme, "Localization for mobile robot teams using maximum likelihood estimation," in *2002 IEEE/RSJ Int. Conf. on Intelligent Robots and Systems*, Lausanne, Switzerland, Sep. 2002, pp. 434–439.

[12] A. Das, J. Spletzer, V. Kumar, and C. Taylor, "Ad hoc networks for localization and control," in *41th IEEE Conf. on Decision and Control*, Dec. 2002, pp. 2978–2983.

[13] A. I. Mourikis and S. I. Roumeliotis, "Performance analysis of multirobot cooperative localization," *IEEE Trans. on Robotics*, vol. 22, no. 4, pp. 666–681, 2006.

[14] X. S. Zhou and S. Roumeliotis, "Determining the robot-to-robot 3d relative pose using combinations of range and bearing measurements (part II)," in *2011 IEEE Int. Conf. on Robotics and Automation*, Shanghai, China, May. 2011, pp. 4736–4743.

[15] N. Trawny, X. S. Zhou, K. Zhou, and S. I. Roumeliotis, "Inter-robot transformations in 3D," *IEEE Trans. on Robotics*, vol. 26, no. 2, pp. 225–243, 2010.

[16] A. Martinelli, "Vision and IMU data fusion: Closed-form solutions for attitude, speed, absolute scale, and bias determination," *to appear in IEEE Trans. on Robotics*, 2011.

[17] A. Franchi, P. Stegagno, and G. Oriolo, "Probabilistic mutual localization in multi-agent systems from anonymous position measures," in *49th IEEE Conf. on Decision and Control*, Atlanta, GA, Dec. 2010, pp. 6534–6540.

[18] A. Franchi, G. Oriolo, and P. Stegagno, "On the solvability of the mutual localization problem with anonymous position measures," in *2010 IEEE Int. Conf. on Robotics and Automation*, Anchorage, AK, May 2010, pp. 3193–3199.

[19] R. Mahony, T. Hamel, and J.-M. Pflimlin, "Nonlinear complementary filters on the special orthogonal group," *IEEE Trans. on Automatic Control*, vol. 53, no. 5, pp. 1203–1218, 2008.

[20] P. Martin and E. Salaün, "The true role of accelerometer feedback in quadrotor control," in *2010 IEEE Int. Conf. on Robotics and Automation*, Anchorage, AK, May 2010, pp. 1623–1629.

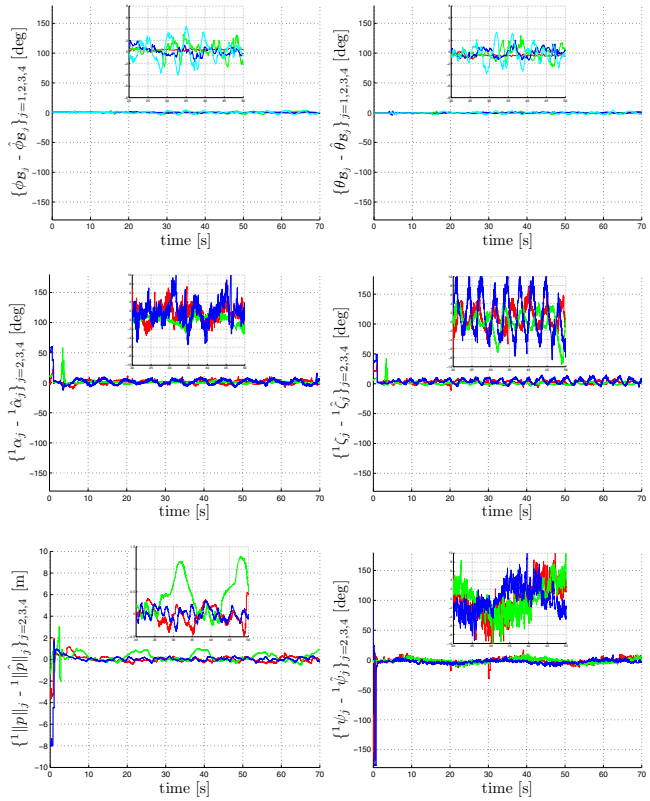


Fig. 6: First experiment. First row: errors on roll and pitch estimates for $A_1, \ldots, A_4$ computed by the complementary filters. Second and third row: errors on azimuth, zenith-distance, distance and yaw estimates for $A_2, A_3, A_4$ computed by the particle filters of $A_1$. Each plot contains a zoom for $t \in [20, 50]$ s.

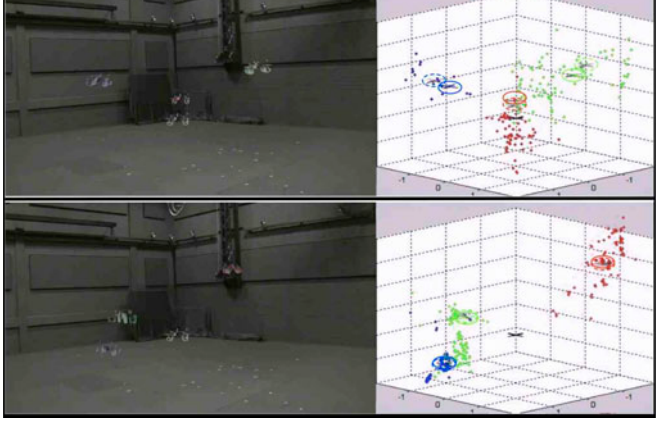

Fig. 7: Two snapshots from the first experiment. On the left, the scene as seen by a fixed camera. On the right, the estimates computed by the filters at the same time instants. The dots represent the best 100 particles. For each quadrotor, the solid circled cross represents the best particle, while the dashed circled cross represents the ground truth. The first snapshot is taken at the very beginning of the experiment, while in the second snapshot the relative distances among the robots have already been retrieved.

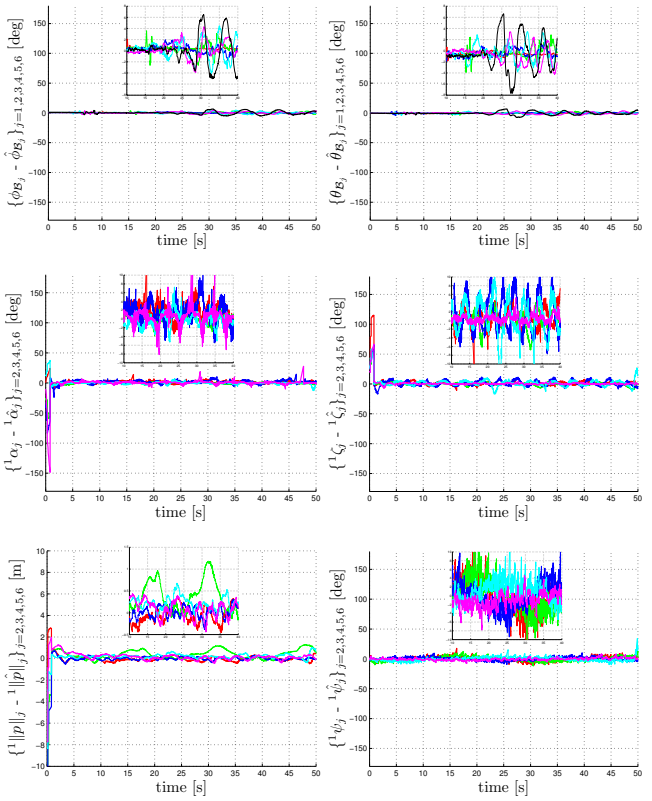


Fig. 8: Second experiment. First row: errors on roll and pitch estimates for $A_1, \ldots, A_6$ computed by the complementary filters. Second and third row: errors on azimuth, zenith-distance, distance and yaw estimates for $A_2, \ldots, A_6$ computed by the particle filters of $A_1$. Each plot contains a zoom for $t \in [10, 40]$ s.

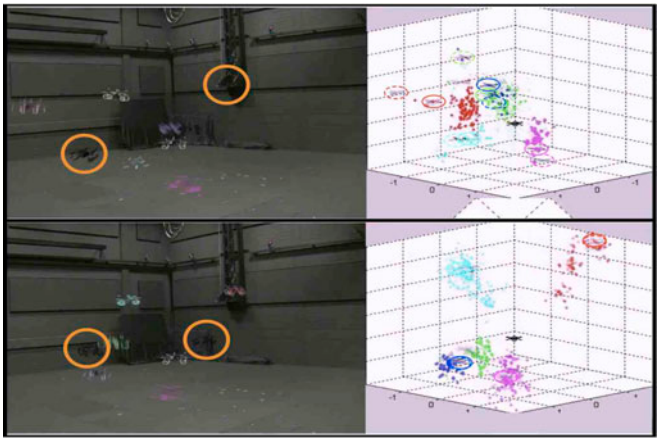

Fig. 9: Two snapshots from the first experiment. On the left, the scene as seen by a fixed camera; the circled quadrotors act as false positives and do not communicate with the others. On the right, the estimates computed by the filters at the same time instants. The dots represent the best 100 particles. For each quadrotor, the solid circled cross represents the best particle, while the dashed circled cross represents the ground truth. The first snapshot is taken at the very beginning of the experiment, while in the second snapshot the relative distances among the robots have already been retrieved.